Magnetic targeting of rhodamine-labeled superparamagnetic liposomes to solid tumors: in vivo tracking by fibered confocal fluorescence microscopy

Marie-Sophie Martina, Jean-Paul Fortin, Laure Fournier, Christine Ménager, Florence Gazeau, Olivier Clément, Sylviane Lesieur

▶ **To cite this version:**

Marie-Sophie Martina, Jean-Paul Fortin, Laure Fournier, Christine Ménager, Florence Gazeau, et al.. Magnetic targeting of rhodamine-labeled superparamagnetic liposomes to solid tumors: in vivo tracking by fibered confocal fluorescence microscopy. Molecular Imaging, 2007, 6 (2), pp.140-146. 10.2310/7290.2007.00004 . hal-00162290

HAL Id: hal-00162290
https://hal.science/hal-00162290v1

Submitted on 28 Apr 2023

HAL is a multi-disciplinary open access archive for the deposit and dissemination of scientific research documents, whether they are published or not. The documents may come from teaching and research institutions in France or abroad, or from public or private research centers.

L'archive ouverte pluridisciplinaire **HAL**, est destinée au dépôt et à la diffusion de documents scientifiques de niveau recherche, publiés ou non, émanant des établissements d'enseignement et de recherche français ou étrangers, des laboratoires publics ou privés.

Distributed under a Creative Commons Attribution 4.0 International License

BRIEF ARTICLE

Magnetic Targeting of Rhodamine-Labeled Superparamagnetic Liposomes to Solid Tumors: In Vivo Tracking by Fibered Confocal Fluorescence Microscopy

Marie-Sophie Martina, Jean-Paul Fortin, Laure Fournier, Christine Ménager, Florence Gazeau, Olivier Clément, and Sylviane Lesieur

Abstract

Polyethylene glycol (PEG)ylated and rhodamine-labeled liposomes loaded with maghemite nanocrystals provide a novel nanoscaled hybrid system for magnetic targeting to solid tumors in possible combination with double in vivo imaging by fluorescence microscopy and magnetic resonance imaging (MRI). Human prostate adenocarcinoma tumors implanted in mice were used as a system model. A magnetic field gradient was produced at the tumor level by external apposition of a magnet. Noninvasive fibered confocal fluorescence microscopy was successfully used to track the liposomes in vivo within organs and tumor blood vessels. Active targeting to the magnet-exposed tumors was clearly shown, in agreement with previous MRI studies. The liposomes were driven and accumulated within the microvasculature through a process that preserved vesicle structure and content.

PROGRESS IN CANCER THERAPY depends more and more on the development of noninvasive systems for selective delivery of drugs, biomarkers, or diagnostic agents into malignant tissues and cells, with minimal systemic side effects.[1–4] For this purpose, intravascular nanovectors and targeting strategies have been extensively investigated, especially during the last decade.[5–8] Lipid vesicles or liposomes undoubtedly rank among the most widely used systems.[9,10] Highly biocompatible, liposomes can be easily prepared to a defined size, in the range of a few hundred nanometers. They can transport amphiphilic or hydrophobic substances within their bilayers, as well as hydrophilic species encapsulated within their internal aqueous compartment. Encapsulation protects the loaded species against degradation by the surrounding biologic medium and contributes to reducing their toxic effects. Once introduced into the blood circulation, their passive accumulation in sinusoidal tissues such as liver, spleen, and bone marrow can be partly avoided by grafting hydrophilic polymers onto their surface.[11–13] Coating by poly(ethylene glycol) (PEG) is notably effective in sterically stabilizing liposomes and reduces their uptake by mononuclear phagocytes.[10,14] The so-called stealth® liposomes (100–200 nm in diameter) can cross the endothelium of blood vessels and, to a certain extent, can accumulate in solid tumors[15–17] but generally not to a sufficient extent for therapeutic efficacy.

Active targeting of PEGylated liposomes to or into diseased tissues and cells indeed remains a challenge. One of the first strategies used for this purpose consisted of coupling targeting ligands such as antibodies or peptides to the distal end of the PEG chains to promote a specific liposome-cell association.[10,18–20] The present report focuses on an alternative and/or complementary strategy based on magnetic force driving. This technique has been successfully used for tumor targeting of anticancer drugs bound to magnetic nanoparticles.[7,21–23] We render liposomes magnetic by loading them with a magnetic nanomaterial. We recently developed hybrid systems

From Laboratoire de physico-chimie des systemes polyphases, UMR CNRS 8612, Université Paris-Sud, Faculté de pharmacie, F-92296 Châtenay-Malabry cedex, France; Laboratoire des liquides ioniques et interfaces charges, UMR CNRS 7612, Université Pierre et Marie Curie, Paris cedex, France; Laboratoire de recherche en imagerie, INSERM U494, Faculté de médecine Necker enfants malades, Paris, France; and Laboratoire des milieux desordonnes et heterogenes, CNRS UMR 7603, Université Paris 6 & 7, Paris, France.

This work was supported by a grant from the Ministry of Research in France, Centre National de la Recherche Scientifique (CNRS), and Action Concertée Incitative (ACI) NR 145 (Programme Interdisciplinaire Imagerie du Petit Animal; ACI Nanoscience et Nanotechnologie).

Address reprint requests to: Sylviane Lesieur, Laboratoire de physico-chimie des systemes polyphases, UMR CNRS 8612, Université Paris-Sud, Faculté de Pharmacie, 5 rue Jean-Baptiste Clément, F-92296 Châtenay-Malabry cedex, France; e-mail: sylviane.lesieur@cep.u-psud.fr.

DOI 10.2310/7290.2007.00004

© *2007 BC Decker Inc*

composed of superparamagnetic nanocrystals of maghemite (γ-Fe_2O_3) encapsulated within PEGylated unilamellar phospholipid vesicles referred to as magnetic fluid–loaded liposomes (MFLs).[24,25] An in-depth characterization of these structures has shown their relevance as long-circulating T_2 contrast agents for magnetic resonance imaging (MRI) in vivo.[25] A subsequent study confirmed their feasibility in targeting MFLs and accumulating their content into solid tumors after intravenous injection and apposition of an external magnet onto the targeted anatomic region.[26] Our previous animal experiments were performed on mice bearing two laterally implanted human prostate adenocarcinoma (PC3) tumors. MRIs of magnet-exposed tumors have been used as proof of active accumulation of the iron oxide nanoparticles into the malignant tissue, whereas histologic analysis using iron-specific Perls coloration has confirmed significant concentrations of particles within the tumor microvasculature.[26]

At this stage of the work, it became of critical importance to prove that the structural integrity of the MFL membrane was preserved during magnetic force driving up into the tumor tissue. This point is essential to envisage further therapeutic use of MFLs, for instance, by encapsulating anticancer drugs concurrently with the magnetic fluid, and to ensure that the drug reaches the target. The novelty in the present work is to attach onto the surface of the liposomes the fluorescent dye rhodamine, which then enables fluorescence detection of the lipid bilayers. Therefore, rhodamine-labeled MFLs (Rho-MFLs) provide an original nanosystem for double in vivo imaging that combines fluorescence detection with fiberoptics and MRI.

In this study, to track MFLs in vivo within blood circulation, we selected a recently developed and powerful device combining confocal fluorescence microscopy with fiberoptics (Cellvizio, Mauna Kea Technologies, Paris, France). As already shown, Cellvizio enables in vivo in situ microvascular exploration and imaging of intact organs in their native environment, with limited invasiveness and preservation of the physiology of the tissues.[26] Fluorescent MFLs were newly synthesized by incorporating *N*-(lissamine rhodamine B sulfonyl) phosphatidylethanolamine (Rho-PE) in the vesicle bilayer based on egg phosphatidylcholine (EPC) and a distearoylphosphatidylethanolamine derivative of PEG (M = 2000) as a steric stabilizer. The fluorescence and size characteristics of the fluorescent MFLs were investigated before the animal experiments. The same magnetic targeting procedure as that previously reported[26] was applied to PC3 tumor–bearing mice. Time-resolved intravascular visualization of the circulating liposomes was performed in a variety of healthy tissues and in solid tumors in the presence and absence of a magnetic field gradient.

Materials and Methods

Chloroform solutions of EPC, 1,2-diacyl-SN-glycero-3-phosphoéthanolamine-*N*-[methoxy(polyethylene glycol)-2000] (DSPE-PEG_{2000}) and Rho-PE were purchased from Avanti Polar Lipids (Alabaster, AL). Sodium chloride, sodium citrate, and *N*-[2-hydroxyethyl]piperazine-*N*′-[2-ethanesulfonic acid] (HEPES) were provided by Sigma (St. Louis, MO). The buffer used was 108 mM NaCl, 20 mM sodium citrate, 10 mM HEPES, pH 7.4, and 285 mOsm (measured with a cryoscopic micro-osmometer, Bioblock Scientific, Illkirch, France).

Nanocrystals of maghemite (γ-Fe_2O_3) were synthesized according to a procedure already described.[24,27] Final adjustment of both aqueous medium and maghemite concentration (5.4 M Fe(III) by flame spectroscopy) was performed by an ultrafiltration MACROSEP filter, cutoff 50 kDa (Fisher Scientific Labosi, Illkirch, France). Rho-MFLs were prepared, as previously described,[24,25] by hydration of a thin lipid film (EPC: DSPE-PEG_{2000}: Rho-PE; 94:5:1 mol %; 20 mM total lipid) by adding equal volumes of the suspension of maghemite particles and buffer (108 mM NaCl, 20 mM sodium citrate, 10 mM HEPES, pH 7.4 buffer) to get a total lipid concentration of 20 mM. Then they were sequentially extruded (nitrogen pressure $<$ 10 bars, 25°C) through polycarbonate filters with decreasing pore diameters of 0.8 μm/0.4 μm/0.2 μm (PORETICS, Osmotics, Livermore, CA). Nonentrapped maghemite particles were removed by gel exclusion chromatography performed with a 0.4 $\times$ 5.8 cm Sephacryl S1000 superfine (Pharmacia, Amersham Bioscience, Orsay, France) microcolumn (TERUMO 1 mL syringe) saturated with EPC: DSPE-PEG_{2000} (95:5 mol %) liposomes prepared in a manner similar to that of Rho-MFLs but empty of maghemite. The eluent was the buffer used for liposome preparation. Final Fe(III) concentration was measured by flame spectroscopy. The final lipid concentration was determined by an enzymatic assay (Phospholipides Enzymatiques PAP 150, Biomérieux, Lyon, France). A maximum variation of $\pm$ 0.5 mM lipids was found between the liposome preparation before extrusion (20 mM concentration by weight) and the extruded liposome preparation recovered after chromatography.

Hydrodynamic diameters of liposomes were determined by quasielastic light scattering (QELS) with a Nanosizer apparatus (N4 MD, Coultronics, Margency, France) at 25°C and a 90° scattering angle and using size distribution

processor analysis (total lipid concentration 0.15 mM). Mean hydrodynamic diameters d_h were calculated from the measured mean translational diffusion coefficient D of the particles according to the Stokes-Einstein law for spherical and noninteracting particles: $d_h = k_BT/3\pi\eta D$ (k_B, Boltzmann constant; η viscosity of the aqueous medium).

Fluorescence emission spectroscopy was carried out on a spectrofluorimeter (Fluorolog Spex FL1T11, Jobin Yvon, Longjumeau, France) connected to a computer. Samples (0.2 mM total lipids) were placed in 1 cm path quartz cells thermostated at 25°C.

Confocal fluorescence microscopy was performed with a CLSM 510 microscope (Zeiss, Le Pecq, Germany) coupled to an LSM 5 Image Browser (Zeiss) equipped with an air-cooled ion laser providing excitation light at 488 and 543 nm. Images were obtained by using a Plan Apochromat (Zeiss) 63×/1.4NO oil objective lens.

Animal experiments were performed in accordance with INSERM animal protection guidelines and were approved by local governmental authorities. Human prostate adenocarcinoma cells (PC3) were a gift from Dr. M. F. Poupon (URA 620, CNRS, Institut Curie, Paris). As already described,[26] two subcutaneous PC3 tumors were implanted on each flank of four male Swiss nude mice (28–34 g) (Iffa Credo, l'Arbresle, France) by an injection of a suspension of 1.5×10^6 cells in 0.2 mL of phosphate-buffered saline. Tumors, measuring 7 × 7 mm in average, developed within 25 days. The mice were anesthetized by intraperitoneal injection of 0.1 mL/10 g of a 4:1 vol/vol mixture of xylazine 2% (Rompum, Bayer, Leverkusen, Germany), that is, 16 mg/kg, and ketamine 500 (Imalgene, Rhône Mérieux, Lyon, France), that is, 100 mg/kg, and their body temperature was kept at the physiologic level using a heating lamp. Rho-MFL dispersion was twice diluted with buffer and injected into the caudal vein (200 µL, 10 mM total lipids, 26 mM [Fe(III)]) so that the injected iron concentration was 9.1 mg Fe/kg of mouse, far below the acute toxic dose for mice (50 g Fe/kg; intravenous).[28] Then mice were surgically prepared for visualization in vivo in situ: a 1 cm–long buttonhole slit was performed through the skin above each organ or tissue to visualize the mesentery, liver, kidneys, or tumors. In magnetic targeting experiments, before any injection, a cylindrical magnet (diameter 14 mm; thickness 5 mm; magnetic field gradient of 30 T/m at 1 mm from the magnet surface) was fixed on the external side of one of the two tumors by cyanoacrylate glue and maintained by a flexible strip until observation.

Fibered confocal fluorescence microscopy (Cellvizio) used a 488 nm laser source and a collection 500 to 650 nm bandwidth. The experimental device is shown in Figure 1. An optical fiber miniprobe, with a diameter of 0.3 mm (ref. S-0300-07), collected light from the observation site and conveyed it toward a specific imaging device. This probe provided direct microvascular images immediately below the surface of the biologic tissue down to a depth of 15 µm, with lateral resolution of 5 µm, as calibrated by Cellvizio providers.[29] The total field of view was 400 × 280 µm. The probe was maintained in contact with the surface of the organs using a specially designed device (see Figure 1) while tissues were regularly hydrated by a saline buffer (physiologic serum; 0.9% NaCl).

The fluorescence intensity of the images was analyzed using *Scion Image* software (Scion Corporation, Frederick, MD). An intensity threshold (120–254 grey level on a 256 greyscale image) was adjusted to analyze Rho-MFL accumulation in terms of the total area covered by Rho-MFLs. This area was then normalized to the microscope field of view and expressed as follows:

$$\text{Normalized Area (\%)} = \frac{100 \times \text{Total area above intensity threshold}}{\text{Total field of view}}$$

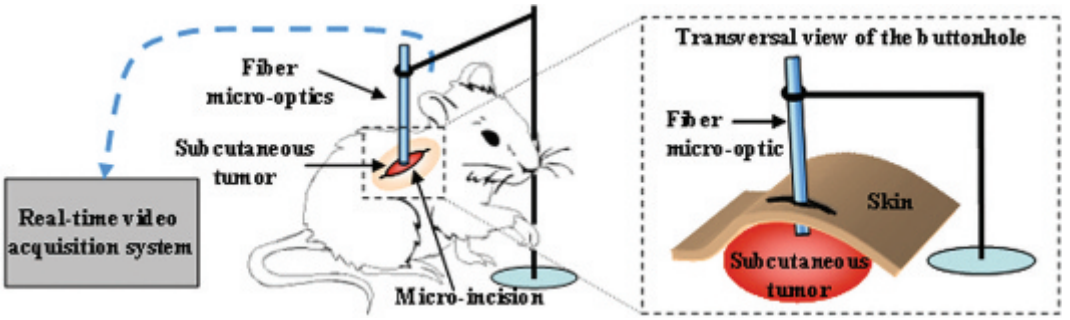

Figure 1. Cellvizio device.

Results and Discussion

Rho-MFLs were homogeneous in size, with a unimodal hydrodynamic diameter distribution centered on 180 ± 25 nm from QELS. Iron loading was 2.6 mol of iron per mole of lipids (20 mM total concentration), corresponding to a local concentration of 2.7 M Fe(III) in the internal aqueous volume of the vesicles. Confocal fluorescence microscopy image of Rho-MFLs revealed individual particles that were rather monodisperse in size (Figure 2A), as checked by the image of 200 nm beads of a standard latex obtained in the same conditions (Figure 2B). The liposomes are seen with an apparent size higher than their effective hydrodynamic diameter of 180 nm, which arises from a superimposed Rayleigh scattering effect.

Rho-MFLs exhibited the same size, structural characteristics, and stability as those of nonlabeled MFLs previously studied.[25,26] The in vivo behavior of the Rho-MFLs investigated here should be directly transposed to nonlabeled MFLs. Figure 3 shows the fluorescence emission spectrum of Rho-MFLs in buffer. It presents a rather symmetric peak in the 560 to 620 nm wavelength range, pointing out that the fluorescence properties of the lipid probe Rho-PE used to label MFLs are not affected by the presence of maghemite inside the liposomes. The emission band appears to be suitable for using the Cellvizio device, the collection bandwidth of which ranges from 500 to 650 nm.

The Cellvizio system provided clear in-focus images of thin tissue sections within the sample tissues. The signal was corrected for both spatial distortion and optical fiber signal modulation so that media without any fluorescent material appeared to be completely dark. Prior to Rho-MFL administration, no intrinsic autofluorescence of vessels and tissues was observed in both the organs and solid tumors so that any subsequent fluorescence signal could not arise otherwise from Rho-MFLs. Images were recorded in real time at a rate of 12 images/s. In the absence of a magnetic field gradient (no magnet on the tumors), as soon as injected into the caudal vein of the mice and during the following 8 hours, liposomes were clearly detected as fluorescent particles circulating within the vessels of the external walls of the mesentery, liver, and kidneys. First, this shows that Rho-PE is appropriate for detection in total blood, as previously described.[30,31] Second, the liposomes were continuously moving and did not adsorb onto the vessel walls. Figure 4 shows representative images recorded 2 hours after intravenous administration. Fluorescence arising from circulating liposomes shows the vascular architecture of the organs, mesentery veins (see Figure 4A), liver sinusoids (see Figure 4B), and kidney arterioles (see Figure 4C). The presence of notable concentrations of in-blood circulating MFLs within the mesentery vasculature several hours after injection was evidence of the in vivo stealthiness of the PEG-coated liposomes. As our previous MRI experiments have shown, the 8-hour persistence of numerous iron oxide particles in the blood after MFL injection[25] confirms that MFLs circulate in blood as intact vesicles, without loss of magnetic fluid. Circulating liposomes could be similarly seen in the tumors (see Figure 4D), but they were sparser, likely owing to the dense and heterogeneous vascular network within the tumoral tissue and its irregular blood flow. The tumoral vessel network of PC3 xenografts was already visualized with Cellvizio by injecting a fluorescein isothiocyanate–500 kDa dextran solution,[32] which revealed a rich, superficial, but irregularly distributed vasculature.

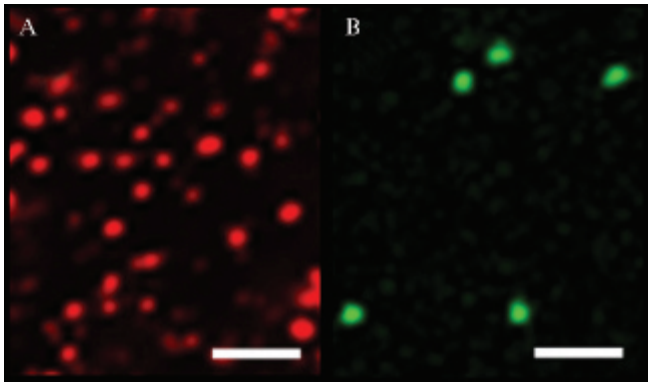

Figure 2. Confocal fluorescence microscopy images of (*A*) rhodamine-labeled magnetic fluid–loaded liposomes (5×10^{-2} mM total lipid; 1 mol % of rhodamine-phosphatidylethanolamine) and (*B*) 200 nm beads of a standard latex (Tetraspeck 0.22 μm, Molecular Probes, Eugene, OR). Incident ion-laser wavelength: 543 nm and 488 nm. White bars represent 2.5 μm.

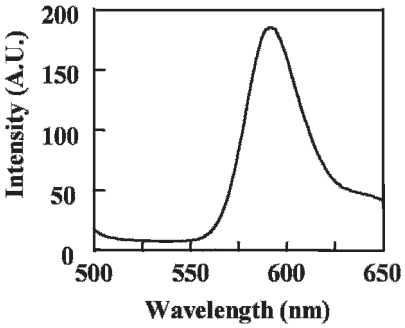

Figure 3. Fluorescence emission spectrum of rhodamine-labeled magnetic fluid–loaded liposomes (0.2 mM total lipids; 1 mol % rhodamine-phosphatidylethanolamine) in buffer at 25°C recorded at an excitation wavelength of 488 nm.

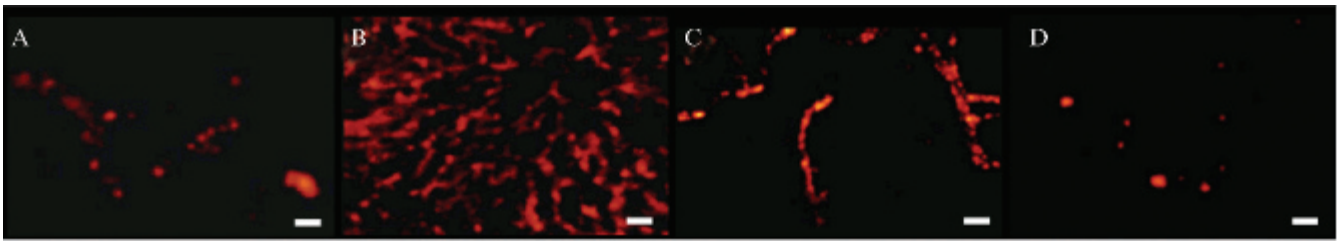

Figure 4. Fibered confocal fluorescence microscopy images obtained with the surface probe on the external wall of the mesentery (*A*), liver (*B*), and kidney (*C*) and PC3 tumor (*D*) 2 hours after intravenous injection of 200 μL rhodamine-labeled magnetic fluid–loaded liposome dispersion (10 mM total lipids, 26 mM [Fe III]) and without magnet exposure. White bars represent 28 μm.

Representative images related to magnetic targeting experiments are shown in Figure 5. The optical probe was placed on the surface of the PC3 tumors by means of a minimal incision in the skin, which preserves the integrity of the tissue. Images were acquired 8 hours after intravenous injection of Rho-MFLs. The control tumors exhibited few fluorescence signals, as shown in Figure 4A. In contrast, the tumors exposed to the magnetic field gradient contained a number of liposomes, as depicted by the strong fluorescence intensity detected within the vessels (see Figure 5B). This demonstrated that in-blood persistent liposome structures were driven by the magnet, via the blood vessels, into the tumor microvasculature. Magnetic driving could occur only because the magnetic fluid was still associated with the liposomes. Moreover, our previous MRI studies on the same animal model and experimental conditions have also provided evidence of increases in the iron oxide density inside the magnet-exposed tumor.[26] Taking into account both fluorescence and MRI observations, it can be concluded that active targeting into solid tumors under a magnetic field gradient preserves the initial vesicle structure and magnetic content of MFLs. A tentative estimate of the magnetic targeting efficacy was provided by quantifying the fluorescence of the video images (see Figure 5C). Rho-MFL fluorescence detected in the magnet-exposed tumors was 20-fold higher than that found in control tumors. This was in agreement with MRI-quantified distribution of the MFL-carried iron oxide particles.[26]

To prove that the accumulation of MFLs is magnetically induced, we imaged the circulatory system after the removal of the magnetic field. Figure 6 presents a time-resolved sequence of images (video film is accessible as supporting information), which depict the movement of liposomes in a tumor capillary 20 minutes after removal of the magnet. The arrows point out the circulatory pathway of the liposomes. Clearly, liposomes are again freely circulating along the vessels, in favor of at least partial reversibility of their magnetically induced accumulation process.

In this work, however, enhanced cell internalization of the liposomes using magnetic guidance of Rho-MFLs was not shown. This would lead to increased MFL accumulation within the microvasculature of the malignant tissue, raising the probability of passive extravasation to the perivascular regions of the tumor. Moreover, as liposomes accumulate in their intact form, MFL clusters may act as a reservoir of contrast or imaging agents, which could leak out of the vesicles over time, prolonging effective delivery to the tumor site. With respect to the magnetic fluid, 8 nm iron oxide nanoparticles can be eliminated by the natural iron pathway.[33]

In summary, this work entailed the preparation, characterization, and successful magnetic targeting toward

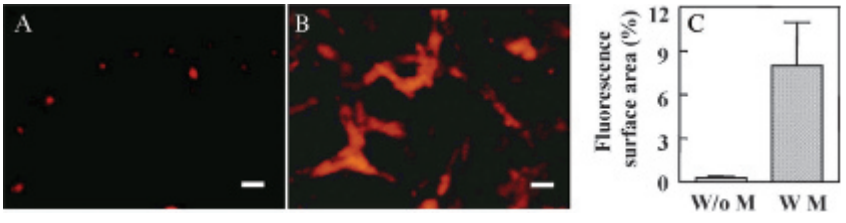

Figure 5. Fibered confocal fluorescence microscopy images obtained with the surface probe on the external wall of PC3 solid tumors, 8 hours after intravenous injection of 200 μL rhodamine-labeled magnetic fluid–loaded liposome dispersion (10 mM total lipids, 26 mM [Fe III]). *A*, Control tumor without magnet exposure; *B*, 8-hour magnet-exposed tumor. Fluorescence surface area counting in the microvasculature of control tumors (without magnet exposure; W/o M) and tumors submitted to the magnetic field gradient (with magnet exposure; W M); $n = 3$ (number of analyzed area/movie = 5) (*C*). White bars represent 28 μm.

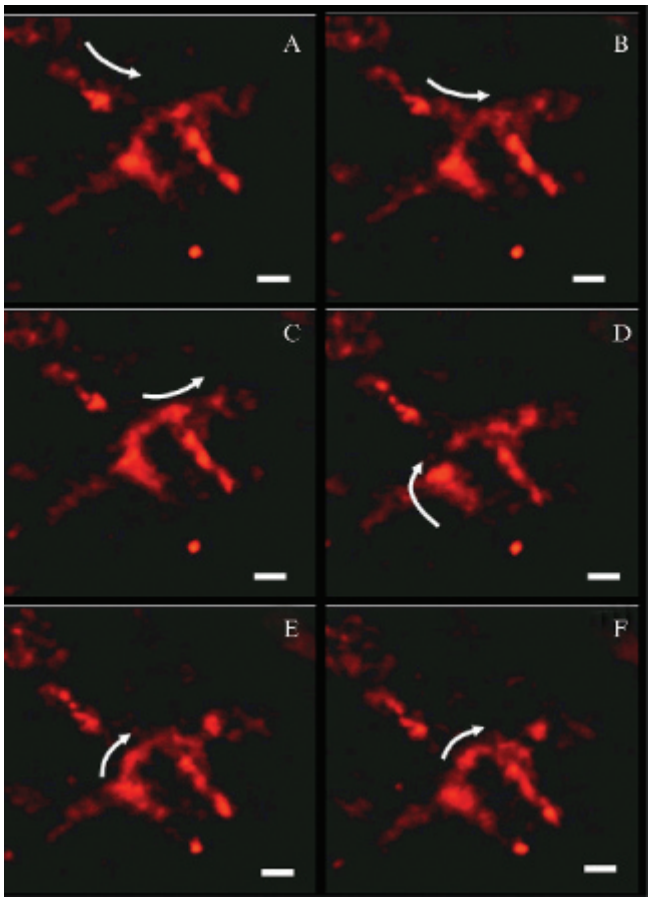

Figure 6. Time-resolved fibered confocal fluorescence microscopy images of rhodamine-labeled magnetic fluid–loaded liposomes within the microvasculature of a PC3 solid tumor first exposed for 8 hours to a magnetic field gradient and second observed 20 minutes after magnet removal (the images here). *A* to *F* were recorded every 0.16 seconds. The *arrows* indicate circulation pathways of the fluorescent liposomes along the vessels. White bars represent 28 μm.

solid tumors of PEGylated, Rho-labeled, and superparamagnetic liposomes. Imaging of fluorescent liposomes had been carried out in vivo, by classic fluorescence videomicroscopy.[17,30,31,34,35] Otherwise stated, our experiments constitute the first visualization of circulating liposomes within the vasculature of different organs in the same living animal, with minimal invasiveness, no previous treatment, and no injection of any other blood marker.

It was clearly demonstrated here that the structural integrity of the liposome membrane is preserved during magnetic targeting until tumor tissue. Rho-MFLs should constitute a powerful tool in cancer therapy, not only for simple diagnosis but also for active targeting of drugs and hyperthermia treatment on the basis of the superparamagnetic properties of the iron oxide particles.[36] They transport two imaging agents: maghemite nanocrystals, which act as efficient magnetic resonance contrast agents, and Rho-PE, which is a suitable lipid marker for in vivo fluorescence microscopy. Thus, diagnosis and delivery control can be based on both MRIs and fiberoscopy images. Further studies focusing on pharmacokinetics, biodistribution, and therapeutic applications on animal models are under way.

Acknowledgments

We thank D. Talbot for iron dosage and V. Nicolas (Plateau Technique - Imagerie Cellulaire IFR141) for technical assistance and performance of the confocal studies, as well as C. Vaysettes for helping in the animal experiments.

References

1. Torchilin VP. Drug targeting. Eur J Pharm Sci 2000;11 Suppl 2:81–91.
2. Feng S-S, Chien S. Chemotherapeutic engineering: application and further development of chemical engineering principles for chemotherapy of cancer and other diseases. Chem Eng Sci 2003; 58:4087–114.
3. Matthews SE, Pouton CW, Threadgill MD. Macromolecular systems for chemotherapy and magnetic resonance imaging. Adv Drug Deliv Rev 1996;18:219–67.
4. Okuhata Y. Delivery of diagnostic agents for magnetic resonance imaging. Adv Drug Deliv Rev 1999;37:121–37.
5. Allen TM. Ligand-targeted therapeutics in anticancer therapy. Nature 2002;2:750–63.
6. Harris JM, Chess RB. Effect of PEGylation on pharmaceuticals. Nature 2003;2:214–21.
7. Häfeli UO. Magnetically modulated therapeutic systems. Int J Pharm 2004;277:19–24.
8. Neuberger T, Schöpf B, Hofmann H, et al. Superparamagnetic nanoparticles for biomedical applications: possibilities and limitations of a new drug delivery system. J Magn Magn Mater 2005;293: 483–96.
9. Andresen TL, Jensen SS, Jorgensen K. Advanced strategies in liposomal cancer therapy: problems and prospects of active and tumor specific drug release. Prog Lipid Res 2005;44:68–97.
10. Sapra P, Allen TM. Ligand-targeted liposomal anticancer drugs. Prog Lipid Res 2003;42:439–62.
11. Needham D, Hristova K, McIntosh TJ, et al. Polymer-grafted liposomes: physical basis for the "stealth" property. J Liposome Res 1992;2:411–30.
12. Allen TM, Hansen CB, de Menezes DEL. Pharmacokinetics of long-circulating liposomes. Adv Drug Deliv Rev 1995;16:267–84.
13. Woodle MC. Controlling liposome blood clearance by surface-grafted polymers. Adv Drug Deliv Rev 1998;32:139–52.
14. Papahadjopoulos D, Allen TM, Gabizon A, et al. Sterically stabilized liposomes: improvements in pharmacokinetics and antitumor therapeutic efficacy. Proc Natl Acad Sci U S A 1991; 88:11460–4.

15. Harashima H, Kiwada H. Liposomal targeting and drug delivery: kinetic consideration. Adv Drug Deliv Rev 1996;19:425–44.
16. Maruyama K, Ishida O, Takizawa T, Moribe K. Possibility of active targeting to tumor tissues with liposomes. Adv Drug Deliv Rev 1999;40:89–102.
17. Unezaki S, Maruyama K, Ishida O, et al. Direct measurement of the extravasation of polyethyleneglycol-coated liposomes into solid tumor tissue by the in vivo fluorescence microscopy. Int J Pharm 1996;144:11–7.
18. Forssen E, Willis M. Ligand-targeted liposomes. Adv Drug Deliv Rev 1998;29:249–71.
19. Allen TM, Moase EH. Therapeutic opportunities for targeted liposomal drug delivery. Adv Drug Deliv Rev 1996;21:117–33.
20. Gabizon A, Shmeeda H, Horowitz AT, et al. Tumor cell targeting of liposome-entrapped drugs with phospholipid-anchored folic acid-PEG conjugates. Adv Drug Deliv Rev 2004;56:1177–92.
21. Goodwin S, Peterson C, Hoh C, Bittner CJ. Targeting and retention of magnetic targeted carriers (MTCs) enhancing intra-arterial chemotherapy. Magn Magn Mater 1999;194:132–9.
22. Lübbe AS, Alexiou C, Bergemann CJ. Clinical applications of magnetic drug targeting. Surg Res 2001;95:200–6.
23. Lübbe AS, Bergemann C, Brock J, McClure DGJ. Physiological aspects in magnetic drug-targeting. Magn Magn Mater 1999;194:149–55.
24. Lesieur S, Grabielle-Madelmont C, Menager C, et al. Evidence of surfactant-induced formation of transient pores in lipid bilayers by using magnetic-fluid-loaded liposomes. J Am Chem Soc 2003;125:5266–7.
25. Martina M-S, Fortin J-P, Ménager C, et al. Generation of superparamagnetic liposomes revealed as highly efficient MRI contrast agents for in vivo imaging. J Am Chem Soc 2005;127:10676–85.
26. Fortin J-P, Martina M-S, Gazeau F, et al. Magnetic targeting of magnetoliposomes in solid tumors monitored by MRI. Radiology 2006;239:415–24.
27. Massart R. US patent 4329241. 1982.
28. Kontoghiorghes GJ. Comparative efficacy and toxicity of desferrioxamine, deferiprone and other iron and aluminium chelating drugs. Toxicol Lett 1995;80:1–18.
29. Cellvizio device. Available at: www.maunakeatech.com. (accessed March 5, 2007).
30. Wu NZ, Klitzman B, Rosner G, et al. Measurement of material extravasation in microvascular networks using fluorescence videomicroscopy. Microvasc Res 1993;46:231–53.
31. Vennemann P, Kiger KT, Lindken R, et al. In vivo microparticle image velocity measurements of blood-plasma in the embryonic avian heart. J Biomech 2006;39:1191–2000.
32. Slide 16/20. Available at: www.maunakeatech.com/flashes/cellvizio_vasc/Index.swf. (accessed March 5, 2007).
33. Weissleder R, Bogdanov A, Neuwelt EA, Papisov M. Long-circulating iron oxides for MR imaging. Adv Drug Deliv Rev 1995;16:321–34.
34. Devoisselle J-M, Begu S, Tourné-Péteilh C, et al. In vivo behaviour of long-circulating liposomes in blood vessels in hamster inflammation and septic shock models—use of intravital fluorescence microscopy. Luminescence 2001;16:73–8.
35. Wu NZ, Da D, Rudoll TL, et al. Increased microvascular permeability contributes to preferential accumulation of stealth liposomes in tumor tissue. Cancer Res 1993;15:3765–70.
36. Ito A, Shinkai M, Honda H, Kobayashi TJ. Medical application of functionalized magnetic nanoparticles. Biosci Bioeng 2005;100:1–11.